Institute of Arctic and Alpine Research
UNIVERSITY OF COLORADO BOULDER

UNIVERSITY OF Southampton

Wave and fluvial discharge interaction along a multichannel delta coastline: A numerical modelling analysis

Matthew Afolabi [mra1u19@soton.ac.uk]

Supervisors: Stephen Darby, Eli Lazarus

University of Southampton, United Kingdom

1. Background

- Coastline morphological evolution along wave-influenced deltas results mainly from the interplay between waves and fluvial processes [1,2].
- While the fluvial agent is the main source of both sediment and water discharges, waves act as the sediment transport agency at the coastline.
- At the river mouth, wave-generated longshore current, interacts with the jet from fluvial discharge.
- The delta river mouth obstructs the longshore sediment transport, a process variably described as the "hydraulic groyne effect"[2,3] or "dynamic diversion"[4,5], ensuring sediment retention and shoreline progradation [4,2].
- In the case of a multi-channel river delta, multiple river mouths create a multiplicity of the 'groyne effect' although coastline morphodynamic evolution may become more complex due to inherent alongshore gradients in sediment transport and deposition.
- Recent numerical model studies [5,6] have explored the interplay between waves and fluvial discharge at a delta river mouth, although fresh insight is currently required regarding interaction of discharge through multiple river mouths with waves and longshore current.
- Therefore, attempt was made in this work to explore, with a numerical model, how delta coastline morphology evolves as a result of wave action along a coastline with two river mouths.

2. Model conceptual framework

- Applying a simple one-line coastline approach as a descriptive framework, longshore sediment transport (LST) along the coastline interacts with the jet of fluvial discharge through the river mouth (**Fig. 1A**). The fluvial jet disrupts the LST causing sediment deposition and shoreline advance in the updrift side of the river mouth along with shoreline erosion in the downdrift side.
- However, the multichannel coastline considered in this work has two river mouths, O_1 and O_2, out of which fluvial discharges R_1 and R_2 input Q_1 and Q_2 (water), and Q_{s1} and Q_{s2} (sediment), respectively, into the coastline (**Fig. 1B**). Longshore currents transport Q_{ls} parallel to the coastline. R_1 interacts with Q_{ls} at O_1 while similar interaction also occurs at O_2. Coastline morphology change, Δy, may be in the form of:
  - Δy_1 (m) which denotes shoreline progradation updrift O_1.
  - Δy_2 (m) which denotes shoreline progradation downdrift O_2.
  - Δy_{mid} (m) which denotes shoreline progradation in the entire section between O_1 and O_2 hereafter referred to as the 'mid-shore'.
- Variable Δy is anticipated under different combination of wave and fluvial discharge interactions along the delta coastline.

3. Methodology

i. Model simulations were undertaken with the Delft3D model which involves coupled hydrodynamic (SWAN) and flow modules.

ii. The simulation period was 27 days with a 2-day model spin-up period and 25 days of morphological changes.

iii. A MORFAC (Morphological Scale Factor) of 90 is employed to optimise the model thus giving an overall simulation period of 2250 days or ~ 6 years.

iv. In the first set of experiments (**wcl01-03**), fluvial discharge is kept constant while wave climate is varied by jointly reducing the significant height and approach angle (**Table 1**). This is because wave energy density is directly proportional to its significant height while waves' LST capacity decreases away from the optimum at ≤45° [3]. These simulations thus provide insight into how changing wave-induced energy alongshore controls the morphology of a deltaic coastline under constant fluvial discharge.

v. In the second set of experiments (**sfd01-03**), fluvial discharge is made to increase first by 50% and subsequently by 100% while wave climate is kept constant at a point of relative maximum effect , (i.e., Hs 1.5 m and 42°, **Table 1**). These simulations give an insight into how the fluvial jets respond to constant wave forcing when discharge is varied between simulations. **Table 1** outlines the numerical model scenarios.

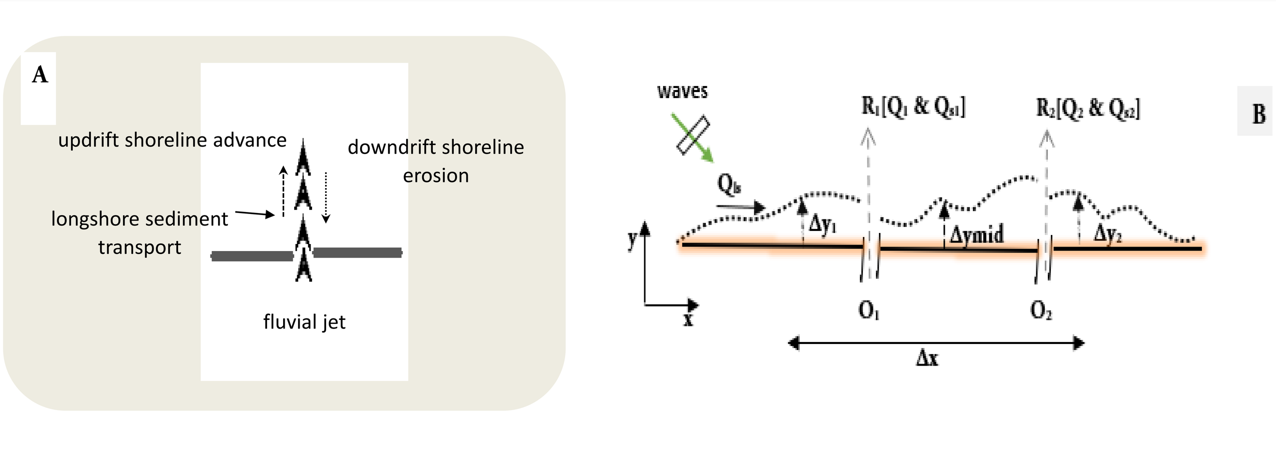

Figure 1: Schematic illustration of waves action against fluvial discharge along the delta coastline

Table 1: Overview of the model simulations

runId	Hs(m)	θ(°)	Q (m³/s)	Qs(kg/s)
		waves		
wcl01	1.5	42	1000	200
wcl02	1.2	28	1000	200
wcl03	1.0	15	1000	200
			fluvial	
sfd01	1.5	42	500	100
sfd02	1.5	42	750	150
sfd03	1.5	42	1500	300

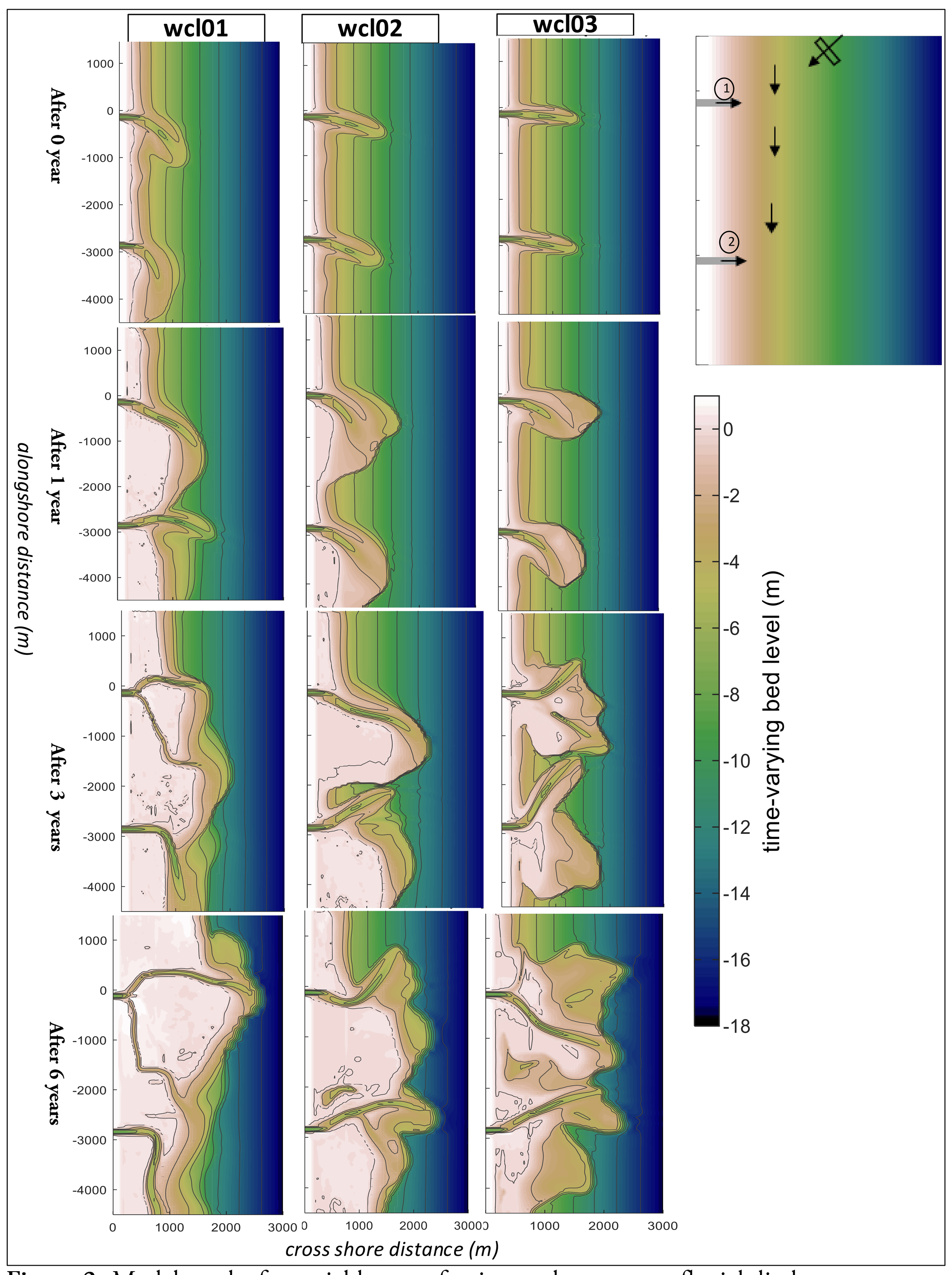

Figure 2: Model results for variable wave forcing under constant fluvial discharge (Q1000/Qs200)

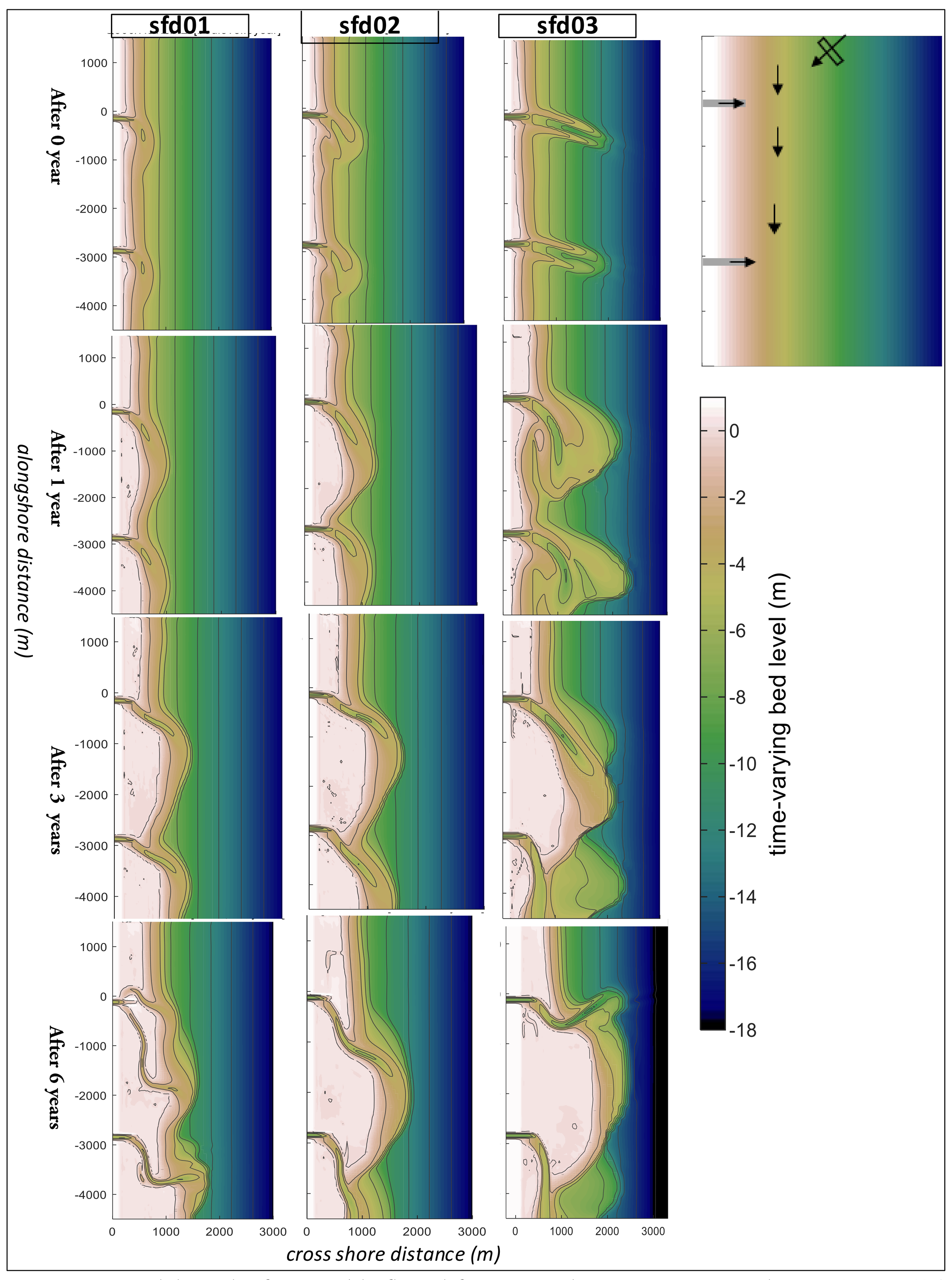

Figure 3: Model results for variable fluvial forcing under constant wave climate (Hs1.5/042°)

4. Preliminary results

- Model results highlight the evolution of the subaerial delta morphology within the 3 distinct segments of the coastline (i.e., updrift of the river 1, mid-shore zone between rivers 1 & 2, and downdrift side of river 2).
- The subaerial delta is defined as the delta area lying at > 0m above the sea level (**Figs 2 & 3**).
- To ascertain the relative influence of waves and fluvial forcing in each model simulation, the concept of jet balance momentum bJm ([6,5]) was employed. This simply relates the momentum jet (M_j) and momentum wave (M_w) using the notation:

$$\frac{M_j}{M_w} = \frac{\rho * Q}{E * n(Cos\theta * Sin\theta) * w}$$

- Where $\boldsymbol{\rho}$ is water density; $\boldsymbol{Q}$ is water discharge; $\boldsymbol{E}$ is wave energy density = $^1/_{16}$ $\rho g H^2$; $\boldsymbol{n}$ is a ratio of group velocity to phase velocity of incoming waves assumed to be 2; **θ** is the incoming wave angle, $\boldsymbol{w}$ is the width of the river mouth, and $\boldsymbol{H_s}$ is the significant wave height. The bJm is analogous to the concept of discharge effectiveness which relates per unit width of fluvial discharge with corresponding nearshore wave power.
- Model simulation **wcl03** (Hs1.0/ θ15°: Q1000/Qs200) records the highest **bJm** while **sfd01** (Hs1.5/ θ42°: Q500/Qs100) has the lowest **bJm (Fig. 4)**.
- Similarly, the delta coastlines in **wcl03** and **sfd01** show the greatest contrast with respect to fluvial jet deflection [**wcl03:** Row1, **sfd01:** Row1] and smoothness of the subaerial delta shoreline [**wcl03:** Row4, **sfd01:** Row4] ; model simulations **sfd03** and **wcl02** show good similarity in their respective delta morphology [**sfd03:** Row4, **wcl02:** Row4] .
- Simulations with varying wave forcing suggest that as waves' capacity to move sediment alongshore increases, the subaerial delta progrades in the mid-shore zone (**wcl01:** Row2) in contrast to reduced wave forcing in which the progradation of the mid-shore zone retards (**wcl03:** Rows2&3). Downdrift jet deflection ensures fluvial sediment spreads close to the coastline whereas as a delta river mouth progrades perpendicular to the shoreline or migrates updrift under increasing influence of the fluvial jet, wave-driven longshore current tends to redistribute fluvial sediment offshore, away from the river mouth[7].
- Results further show that downdrift deflection of fluvial jets enhances subaerial delta progradation (**sfd01:** Rows2-4; **sfd02:** Rows2-4; **sfd03:** Rows3&4,)[7] along with development of spits at the river mouths[6].
- Finally, both sets of simulations indicate that the areal extent of the subaerial delta scales directly with the volume of fluvial discharge (**sfd01-sfd03:** Row 4) as well as the incident wave energy (**wcl01-wcl03:**, Row4).

5. Summary and future work

Future work:

- Attempt will be made to track the passage of sediment across the river mouths.
- Model simulations will also consider varying some geometric properties of the river mouths such as depth, width, and the alongshore distance between the channels.

Summary:

When wave energy is optimised for sediment transport alongshore, subaerial delta progradation is enhanced.

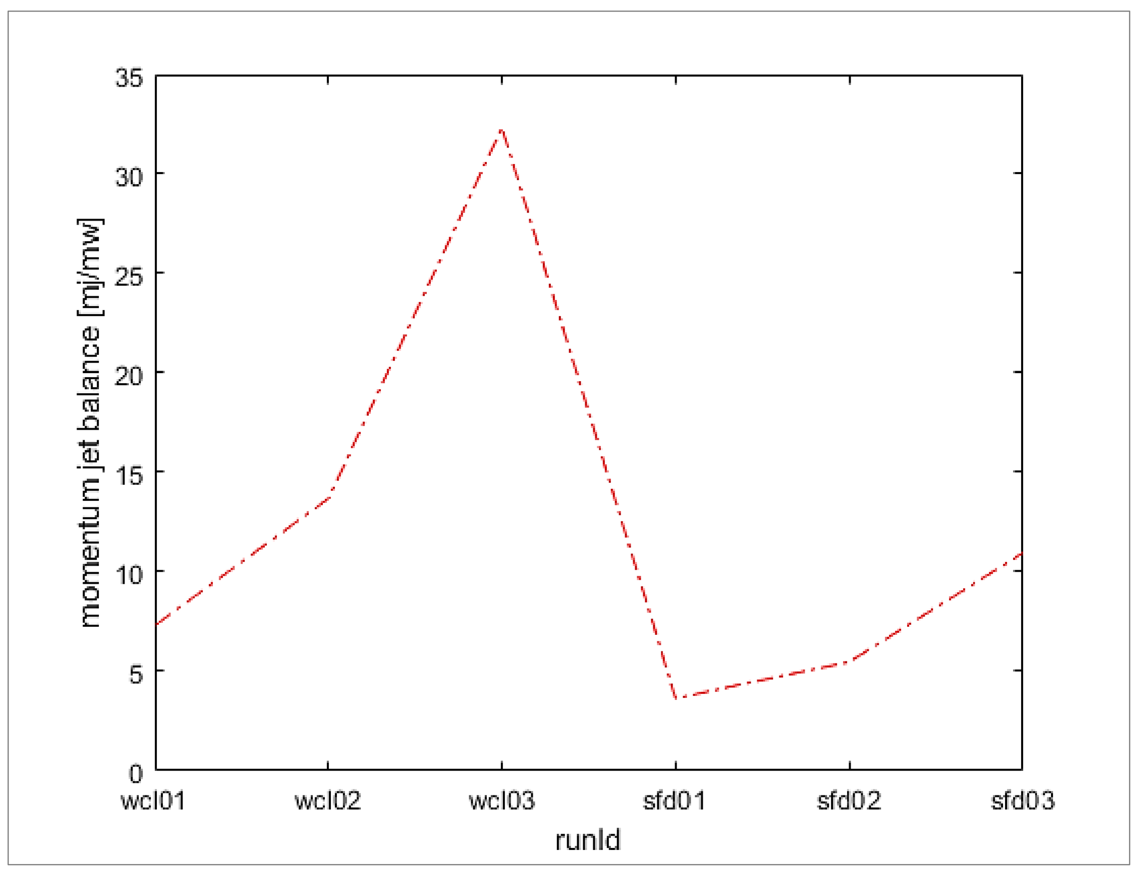

Figure 4: Jet balance momentum (bJm) for the model simulations

PTDF PETROLEUM TECHNOLOGY DEVELOPMENT FUND

6. References

1. **Ashton and Giosan (2011).** Geophy. Res. Let. L13405, doi:10.1029/2011GL047630.
2. **Anthony E. J. (2015).** Mar. Geol., doi.org/10.1016/j.margeo.2014.12.004.
3. **Komar P. (1973).** Geo. Soc. of Ame. Bull., v. 84, p. 2217 222.
4. **Todd T. W. (1968).** *J. Sed. Petrol.,10.1306/74D71A5A-2B21-11D78648000102C1865D.*
5. **Zainescu et al. (2021).** *Front. In Marine Sc. doi: 10.3389/fmars.2021.708258*
6. **Nienhuis et al. (2016).** *J. of Geophy. Res., doi:10.1002/2015JF003780.*
7. **Gao et al. (2020).** *Wat. Reso. Res., doi.org/10.1029/2020WR027298.*